Turbulence Velocimetry of Tangential Fast Imaging Data on QUEST*)

Santanu BANERJEE, Hideki ZUSHI[1)], Nobuhiro NISHINO[2)], Yoshihiko NAGASHIMA[1)], Kazuaki HANADA[1)], Saya TASHIMA, Tsubasa INOUE, Kazuo NAKAMURA[1)], Hiroshi IDEI[1)], Makoto HASEGAWA[1)], Akihide FUJISAWA[1)] and Keisuke MATSUOKA[1)]

IGSES, Kyushu University, 6-1 Kasuga Koen, Kasuga-shi, Fukuoka 816-8580, Japan
[1)]*RIAM, Kyushu University, 6-1 Kasuga Koen, Kasuga-shi, Fukuoka 816-8580, Japan*
[2)]*Mechanical System Engineering, Hiroshima University, Hiroshima 739-8527, Japan*

(Received 7 December 2012 / Accepted 29 May 2013)

A particle image velocimetry technique based on orthogonal dynamic programming is developed to measure the time resolved flow field of the fluctuating structures at the plasma edge and scrape off layer. This non-intrusive technique can provide two dimensional velocity fields at high spatial and temporal resolution from a fast framing image sequence and hence can provide better insights in plasma flow as compared to conventional probe measurements. Applicability of the technique is tested with simulated image pairs. Finally, it is applied to tangential fast visible images of QUEST as a test case to estimate the scrape off layer flow in Ohmic and ECRH driven plasma discharges.

Keywords: particle image velocimetry, fast imaging, turbulence, plasma flow

DOI: 10.1585/pfr.8.2402098

1. Introduction

Plasma edge turbulence remained an area of active research since the early days of fusion science. It plays decisive role in the performance of the plasma core and also cross-field transport of heat and particle fluxes towards the material wall of the plasma confinement chamber. Increasingly, plasma flows at the edge of magnetized plasma deemed imperative in edge turbulence dynamics. Turbulence-driven density fluctuations result in the equilibrium and fluctuating velocity of the coherent structures originating at the plasma boundary. With the advent of density fluctuation diagnostics with high spatial and temporal resolutions, quantitative analysis of such velocities and derived quantities like Reynolds stress, zonal flows etc. becomes feasible. Turbulence imaging diagnostics have been realized in several forms like the beam emission spectroscopy (BES) [1], fast visible imaging [2–5] and microwave reflectometer imaging array [6, 7].

Particle Image Velocimetry (PIV) has proven to be a valuable technique for quantittave estimation of two-dimensional flow structures in experimental fluid mechanics. Application of such a technique to plasma fluctuation images may unveil enormous information of plasma turbulence and flow dynamics. Here we intend to apply the velocimetry technique through orthogonal dynamic programming (ODP) [8, 9] on the tangential fast visible images acquired on the spherical tokamak QUEST. This enables us to evaluate turbulent velocities of the flowing coherent structures at high spatial and temporal resolution.

ODP is a robust technique for searching optical alignments of patterns through the simple realization of cross correlation. So far it has been adapted for BES data [1]. Since the tangential fast images have excellent spatial resolution on the tangency plane, this technique will enable us to track the most intricate features of the flowing coherent structures in the SOL. Further, this will provide a significant improvement over the one dimensional velocity estimates from the probes using wavelet and other time-delay estimation methods. However, it can be noted that ODP relies on optical alignments of various types of patterns as a global transformation between consecutive image strips [8] and thereby it is most likely to track the propagation of the plasma eddies or coherent structures rather than the mean flow.

This paper deals in the development of the velocimetry technique optimized for handling fast visible images. As a test case, the velocimetry code is applied on tangential fast images acquired in the Ohmic-ECRH discharges in the spherical tokamak QUEST. This demonstrates the capabilities of the technique and also helps in optimizing its potential.

2. Orthogonal Dynamic Programming

The procedure is essentially the search of a transformation that relates the consecutive image with the previous

author's e-mail: santanu@triam.kyushu-u.ac.jp
*) This article is based on the presentation at the 22nd International Toki Conference (ITC22).

image in a time series and minimizes the Minkowski distance $L_n = \sum_i \sum_j |I_0(i, j) - I_1(i, j)|^n$ between them. Details of the algorithm are discussed in Ref. [1,8] and can be outline here in the following steps:

(1) Each image of the temporally displaced pair is sliced into several parallel overlapping strips (here along R direction).
(2) Then, for every pair of strips, an optimal match is searched for with displacements allowed only in the slicing direction and identical for all the pixels in the same column in the orthogonal direction (here along Z direction). With the help of dynamic programming a dense field of displacement is computed for every pair of strips by minimizing the distance L_1 between them. The velocity is estimated from the distortion or transformation, in the slicing direction, necessary to minimize the calculated intensity difference. The spatial resolution on the tangency plane and the temporal resolution serve as factors to denote this velocity with respect to real co-ordinates.
(3) The displacement field found in the first step is used to deform the second image relative to the first one. An image $I'(i, j)$ is reconstructed from the $(v_R(i, j), v_Z(i, j))$ displacement field and the image $I_1(i, j)$ as $I'(i, j) = I_1(i + v_Z(i, j), j + v_R(i, j))$. The image $I'(i, j)$ instead of $I_1(i, j)$ is compared and now aligned to $I(i, j)$.
(4) Then, all the above steps are repeated with the slicing performed in the orthogonal (Z) direction and the alignment results are used to update and refine the $(v_R(i, j), v_Z(i, j))$ displacement field.
(5) The whole process is reiterated several times to achieve higher spatial resolution similar to the actual pixel resolution of the image. The width of the strips and the corresponding overlaps are reduced by about $\sqrt{2}$ in each iteration.

The code is first tested with simulated pairs of images. The images contain some patterns which are different in intensities than the background. In the second image the patterns are shifted with known number of pixels (analogous to velocity of the patterns) in both R and Z directions. Figure 1 shows example of such a pair of images and the estimated pixel shifts with the ODP algorithm. Satisfactory match between the simulated shifts and the calculated shifts is obtained.

3. Turbulent Velocity Field Estimation

QUEST is a medium sized spherical tokamak [10] with major and minor radii of 0.68 and 0.4 m, respectively. Diameters of the center stack and the outer wall are 0.2 and 1.4 m with flat divertor plates at b (±1 m) from the mid-plane. In this experiment plasma start up by 8.2 GHz ECRH, is followed by an Ohmic (OH) phase. In the OH phase, plasma current (I_p) value is fed back to the OH coil power supply in order to maintain I_p flat-top at −30 kA. In the middle of the OH phase another ECRH pulse is applied to drive the plasma current thereafter. We focus on this second OH-ECRH phase as strong edge turbulence and poloidal flow is observed at higher density plasma.

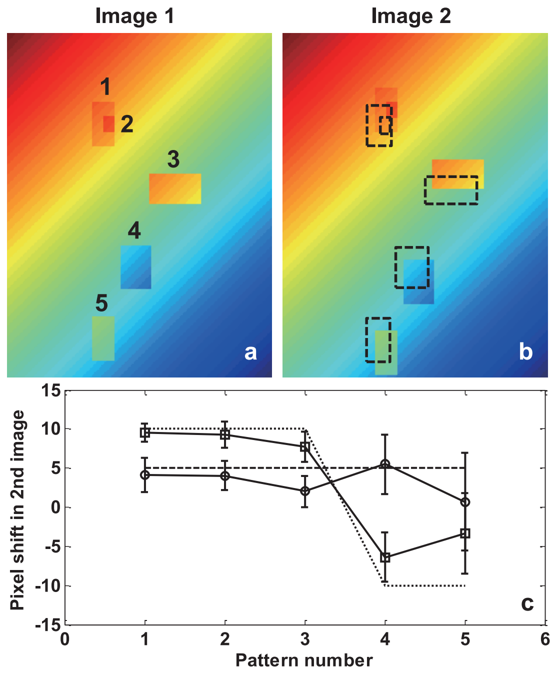

Fig. 1 (a) and (b) shows the pair of images with the patterns numbered as 1~5. In the second image, the patterns are shifted, with the original positions shown in broken rectangles. (c) Dotted and broken lines show the actual shifts in R and Z directions respectively. Squares and circles in the plot represent mean shift for all the pixels within that pattern and the error bars are the $\pm\sigma$ within the pattern in R and Z directions respectively.

A Photron Fastcam SA5 complementary metal oxide semiconductor (CMOS) camera with frame rate of 7000 frames/s at full resolution (1024 × 1024) is used for tangential imaging on the mid-plane of QUEST [4]. Figure 2 shows the top view of QUEST with the tangential field of view (FOV) of the camera and other diagnostics/sub-systems. The camera is operated from the tokamak control room via Gigabit Ethernet, and image acquisition is initiated by an external timing trigger synchronized with the tokamak operational sequence. Image is transferred away from the view port by a 4 m long fiber optic bundle (IG-154) manufactured by Schott. At the back end the camera is connected with the fiber bundle through an image intensifier (Hamamatsu C10880-03C) and a 1:1 relay lens. Each frame is made up of 242 × 242 pixels, and framing rate is 20 kHz. Spatial resolution achieved on the tangency plane is 3.7 mm in both radial (R) and vertical (Z) directions. Comparison with images using H_α filter indicates that observed visible image is mainly attributed to

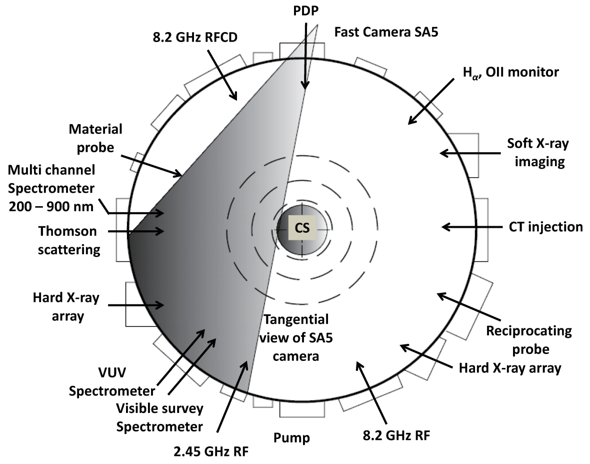

Fig. 2 Top view of QUEST showing the tangential field of view of the fast camera and other diagnostics.

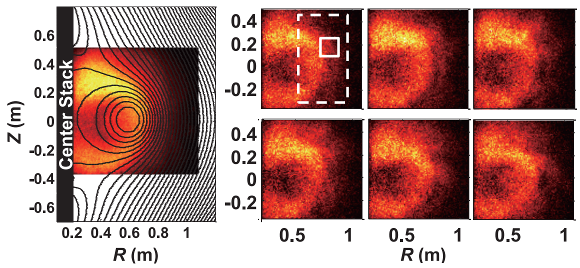

Fig. 3 Image sequence is shown in false color. Images run from left to right and top to bottom and the consecutive images are 50 µs apart. Mean intensity of 175 ms data has been subtracted from the individual frames to highlight the flow at SOL. Solid and broken rectangles on the first image denotes the areas represented in Figs. 4 and 5 respectively. Left panel shows typical image superimposed with flux contours.

H_α emission ($\propto n_0 n_e$). Figure 3 shows the image sequence of a typical shot from the series. Mean intensity of 175 ms data has been subtracted from the individual frames to emphasize the flowing plasma structures at the edge. Also, on the left panel, a typical image is superimposed with the flux contours showing the last closed flux surface (LCFS) and the open field lines in the scrape off layer (SOL).

Line of sight (LOS) integration effect due to the tangential view may hinder the fluctuation assessments. A quantitative evaluation of this effect is carried out under the framework of the TITR code [5, 11]. It is seen that the effect is negligible in the edge and SOL of the plasma as compared to the plasma core as the density and hence the intensity is appreciably smaller in that region. Hence, velocity estimates inside the LCFS seems inconclusive and only velocity at the SOL are reported.

The image sequence tested in this work comprises of 3500 images taken at 20 kHz. The ODP algorithm is extended to the entire time series by selectively taking two consecutive images at each instance. Thus 3499 frames of turbulent velocity field are computed from the intensity images. Figure 4 shows the turbulent velocity maps superimposed on the intensity fluctuations for 8 consecutive frames. The arrows represent magnitude and direction of velocities at a super pixel (5×5 pixels) area for the sake of clarity in representation. Velocity field estimation from a pair of images takes <10 s on a Windows® 7 laptop equipped with Intel® core™ i5 processor and 4 GB RAM. Figure 5 shows $\langle v_R \rangle$ and $\langle v_Z \rangle$, where $\langle\ \rangle$ denotes temporal mean over the image recording window. It can be seen that $\langle v_R \rangle$ remains close to zero with evenly scattered patches of velocities up to $100\,\mathrm{m^{s-1}}$ On the other hand, $\langle v_Z \rangle$ shows up-down anti-symmetry along the poloidal cross section. The top half remains positive while the bottom half neg-

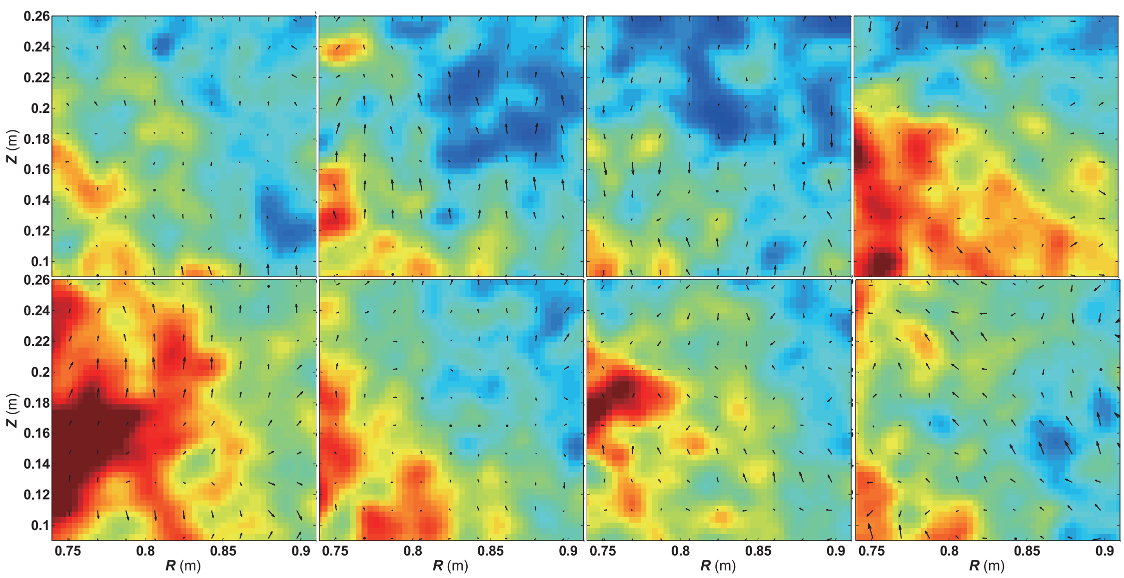

Fig. 4 2D turbulent velocity maps superimposed on the intensity image. Length and orientation of the arrows denote magnitude and direction of the velocity respectively. Each arrow represents velocity at a super-pixel (~3.4 cm^2) for clarity of representation. The frames start at 2.07815 s, run from left to right and top to bottom and the consecutive images are 50 µs apart.

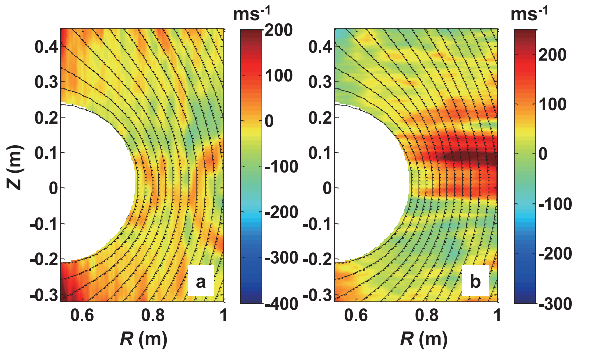

Fig. 5 Mean velocity contours; (a) v_R and (b) v_Z. Colorbar denotes the velocity magnitude in ms^{-1}. SOL Flux contours are overlaid as black dotted solid lines.

ative. Also, $\langle v_Z \rangle$ attains maximum value just above mid-plane ($\sim$300 ms^{-1} at $Z = 0.1$ m). This seems to indicate that the eddies are flowing towards the top and bottom divertor plates after their generation around the mid-plane. The cross field propagation seems much smaller compared to the vertical flow. From the spatial resolution achieved on the tangency plane and the framing rate of the camera, the lowest velocity that can be estimated both along R and Z is $\sim$ 40 ms^{-1}.

4. Discussions

Since the velocities are estimated from the tangential camera images, reflection from the vessel wall, where the FOV of the camera terminates, may introduce artifacts in the velocity estimates. It can be seen from $\langle v_R \rangle$ in Fig. 5, the port structures around mid-plane on the opposite wall are apparent in the velocity field. Fortunately, the absolute magnitudes of such artifacts are not substantially higher in this case. However, for more accurate estimation of velocity fields, the wall reflection needs to be modeled and compensated for in the raw images before applying ODP-PIV as demonstrated in the TITR code [11].

The ODP algorithm is able to search for integer displacements in each iteration. However, sub-pixel resolution can be achieved via interpolation and smoothing while matching the image strips. This algorithm can also be extended to multi-band (i.e. color) images. Such modifications to the basic ODP algorithm can enhance the accuracy and versatility of the technique.

5. Conclusions

A novel method of PIV to construct time varying 2D velocity field $v(R, Z, t)$ from the intensity fluctuations recorded with the tangential fast visible images is developed. ODP proved to be an effective technique to generate the velocity field at a high spatial resolution. Future application of this technique will focus on providing deeper insight in the sheared poloidal flow generation at the plasma edge and SOL. This technique along with the conventional correlation analysis should help in developing a sound physical basis of improved confinement.

[1] G.R. McKee, C. Fenzi, R.J. Fonck and M. Jakubowski, Rev. Sci. Instrum. **74**, 2014 (2003).
[2] S.J. Zweben *et al.*, Phys. Plasmas **9**, 1981 (2002).
[3] R.J. Maqueda *et al.*, Rev. Sci. Instrum. **74**, 2020 (2003).
[4] S. Banerjee *et al.*, Rev. Sci. Instum. **83**, 10E524 (2012).
[5] S. Banerjee *et al.*, Nucl. Fusion **52**, 123016 (2012).
[6] T. Munsat *et al.*, Rev. Sci. Instrum. **74**, 1426 (2003).
[7] Y. Nagayama *et al.*, Rev. Sci. Instrum. **83**, 10E305 (2012).
[8] G.M. Quénot, J. Pakleza and T.A. Kowalewski, Exp. Fluids **25**, 177 (1998).
[9] G.R. McKee, R.J. Fonck, D.K. Gupta, D.J. Schlossberg, M.W. Shafer, C. Holland and G. Tynan, Rev. Sci. Instum. **75**, 3490 (2004).
[10] K. Hanada *et al.*, Plasma Fusion Res. **5**, S1007 (2010).
[11] S. Banerjee and P. Vasu, Nucl. Fusion **49**, 075032 (2009).